Heme Binding Properties of *Staphylococcus aureus* IsdE†

Mark Pluym,§ Christie L. Vermeiren,‡ John Mack,§ David E. Heinrichs,*,‡ and Martin J. Stillman*,§

Department of Chemistry, University of Western Ontario, London, Ontario, Canada N6A 5B7, and Department of Microbiology and Immunology, University of Western Ontario, London, Ontario, Canada N6A 5C1

Received May 18, 2007; Revised Manuscript Received September 4, 2007

ABSTRACT: *Staphylococcus aureus* is the source of a large number of hospital-acquired infections, of which many are serious and can lead to death. Iron is critically important to the survival and growth of the bacterium, and complex, multistep mechanisms are present to fulfill the necessary iron requirement. Isd proteins located on the wall and membrane of *S. aureus* have been proposed to function in heme acquisition. We report characterization of the *S. aureus* heme-binding protein IsdE, the lipoprotein component of a membrane-localized ABC transporter that is believed key to receiving heme from cell wall-anchored Isd proteins. Magnetic circular dichroism (MCD) data, which greatly extend the results from our initial study of IsdE in bacterial cell lysates (Mack, J., Vermeiren, C., Heinrichs, D. E., and Stillman, M. J. (2004) *Biochem. Biophys. Res. Commun. 320*, 781−788), probe the ligand and redox properties of the bound heme. The MCD data show that IsdE, when overexpressed in *E. coli*, binds either ferric or ferrous heme but that the largest fraction is low spin ferrous heme. Studies of mutants allowed identification and characterization of the ligands in the fifth and sixth position on the heme iron as histidine, proximally, and methionine, distally. This histidine-methionine heme-iron ligation is unique to heme transport proteins. The smaller fraction of ferric heme in the protein is not bound by methionine, allowing for access by strong field ligands, such as cyanide. Electrospray ionization mass spectral data are reported for the first time and show that only one heme ligand binds per IsdE protein molecule. These data also show there is little change in the conformation of the protein between the heme-bound and heme-free species, indicating that the heme-free IsdE adopts a structure essentially independent of the heme. The mass spectral data clearly show that IsdE reversibly unwinds under denaturing conditions to form at least two distinct, heme-free conformations.

A surface receptor mediated heme-uptake system has been described in *Staphylococcus aureus*, encoded in a cluster of iron (via Fur)-regulated genes referred to as *i*ron-regulated *s*urface *d*eterminants (*isd*[1]) (*1*). The *isd* locus is conserved in all of the available *S. aureus* genome sequences as well as in several other Gram-positive bacteria including *Listeria monocytogenes*, *Bacillus halodurans*, and *B. anthracis*. The locus includes eight genes, encoded in three iron-regulated transcriptional units, *isdA*, *isdB*, and *isdCDEFsrtBisdG* (*2*). The genes *isdA*, *isdB*, and *isdC* encode cell-wall anchored proteins, characterized by their signal peptides for transport across the cell membrane and C-terminal sorting signal for anchoring to the peptidoglycan cell wall structure. IsdC is anchored to the peptidoglycan by sortase B which is encoded from within the *isd* locus (*2*). The remainder of the genes in this operon have been predicted by sequence similarities to encode a membrane protein (*isdD)*, a lipoprotein (*isdE)*, a permease (*isdF)*, and a cytoplasmic protein (*isdG)*. Encoded at a distinct location in the genome is HarA (for *ha*ptoglobin *r*eceptor), also referred to in the literature as IsdH (*3*). HarA is an iron-regulated cell wall anchored protein with significant similarity to IsdB.

The involvement of the Isd proteins in acquisition of iron from heme or hemeproteins has been documented (*3*−*5*). The acquisition of iron from heme is a complex, multistep process involving the capture of heme and hemoproteins at the bacterial cell surface, removal of the heme moiety (in the case of hemoproteins), and transport into the cytoplasm where heme may be degraded by heme monooxygenases (*6*). The cell-wall proteins IsdB and IsdH are considered to be the primary staphylococcal hemeprotein receptors and have been shown to be involved in capturing hemoglobin (IsdB) and hemoglobin−haptoglobin (HarA/IsdH) at the bacterial cell-surface (*3*, *7*, *8*). Two additional cell-wall anchored proteins, IsdA and IsdC, have been implicated in the binding of heme (*1*, *4*, *5*, *9*−*11*). Significantly, although currently there is no direct evidence, it has been proposed that IsdA mediates the removal of heme from hemeproteins and transfers heme to IsdC, prior to its delivery to the membrane

† This work was supported by an operating grant from the Canadian Institutes of Health Research (CIHR) (to D.E.H), operating and equipment grants from the Natural Sciences and Engineering Research Council (NSERC) of Canada (to M.J.S.), the NSERC Postgraduate Scholarship program (stipend support for M.P), and the Ontario Graduate Scholarship in Science and Technology program (stipend support for C.V.).

* To whom correspondence should be addressed. Phone: D.E.H. (519) 661-3984; M.J.S. (519) 661-3821. Fax: DEH (519) 661-3499; MJS (519) 661-3022. E-mail: deh@uwo.ca; martin.stillman@uwo.ca.

§ Department of Chemistry.

‡ Department of Microbiology and Immunology.

[1] Abbreviations: *isd*, iron-regulated surface determinant; CD, circular dichroism; MCD, magnetic CD; ESI-MS, electrospray ionization mass spectrometry; NEAT, NEAr iron transporter; rIsdA, recombinant IsdA.

10.1021/bi7009585 CCC: $37.00
Published on Web 10/12/2007

for transport into the cell (*12*). In this latter step, two independent ABC-type transporters have been implicated in the transport of heme into the cytoplasm; these have been proposed as the Isd transporters IsdE and IsdF, and the Hts transporter (for *h*eme *t*ransport *s*ystem) (*1*, *10*, *13*). IsdE and HtsA are both predicted to be lipoproteins that function as high-affinity receptors for ligands at the outer surface of the bacterial membrane. They are members of the metal chelate superfamily of binding proteins, characterized by having a bilobed structure with an α helix that connects the two lobes and spans the length of the protein. The ligand binding pocket is formed between the two lobes of the protein.

We have previously demonstrated that, when overexpressed in *E. coli* as a GST fusion protein, IsdE scavenges heme from within the *E. coli* cell. Magnetic circular dichroism (MCD) data on *E. coli* cell lysates containing the overexpressed protein indicated that IsdE bound both ferric and ferrous hemes (*10*). Knowledge of the IsdE:heme stoichiometry and the coordination and electronic properties of the hemes bound in IsdE have not been determined as yet but are crucial in evaluating the role of IsdE in heme transport, as the model of *S. aureus* heme uptake continues to be refined.

In the present study, we have used extensive mass spectrometry and MCD spectroscopy spectral data, coupled with amino acid substitution analyses, to study the heme binding properties of purified recombinant IsdE (rIsdE). We report that the mass spectral data provide exquisite detail of the conformational status of IsdE, showing that heme-bound and heme-free proteins adopt essentially the same structure, whereas IsdE can be reversibly denatured and adopts at least two heme-free conformations, both of which are very much more open than the native structure. The MCD and absorption spectra show that the native, IsdE binds heme as a mixture high spin ferric and low spin ferrous. Mutational analysis identifies histidine and methionine as axial ligands of the heme iron.

EXPERIMENTAL PROCEDURES

Cloning, Overexpression, and Purification of Recombinant IsdE. The *isdE* gene was amplified from the *S. aureus* RN6390 chromosome using oligonucleotides, 5′-GGATCCCAATCTTCCAGTTCTCAA-3′and5′-GGATCCCTATTTTTTATCCTTATAA-3′. The resulting PCR product was subsequently cloned into the GST fusion vector pGEX-2T-TEV generating pGST-IsdE. Overexpression of GST-tagged IsdE in *E. coli* ER2566 (protease-deficient) was achieved by growing plasmid-containing cultures in Luria−Bertani broth (Difco) at 37 °C to an absorbance at 600 nm of approximately 0.8. Isopropyl β-thiogalactopyranoside (IPTG) (0.4 mM) was added, and cultures were grown for a further 20 h at room temperature. Ampicillin (100 μg/mL) was incorporated into all growth media. Bacterial cells were pelleted, resuspended in phosphate-buffered saline (PBS), and lysed in a French pressure cell. Insoluble material was removed by centrifugation at 100 000*g* for 20 min. The GST-IsdE fusion protein was purified by passage of the cell lysate across a 20 mL GSTPrep column (Amersham Biosciences). GST-IsdE was eluted from the column with 10 mM reduced glutathione, 100 mM NaCl, and 50 mM Tris-Cl, pH 9.0. Fusions were cleaved overnight at 4 °C with AcTEV protease (Amersham Biosciences) according to manufacturer's instructions. Cleaved GST was removed by two passages across a GSTPrep column and collection of the flowthrough. During the purification process there are noticeable changes in the color of the protein solutions. This observation is attributed to the gradual oxidation of ferrous heme.

Site-Directed Mutagenesis of IsdE. Site-directed mutagenesis of IsdE was performed using the QuikChange PCR Kit (Invitrogen), with *Pfu* Turbo polymerase and pGST-IsdE or pGST-Y61A as a template. Oligonucleotides: 5′-ATTTTACGATTACCAGCCGGAATGCCT-3′, 5′-AGGCATTCCGGCTGGTAATCGTAAAT-3′, were used to generate the H229A mutation and 5′-AAACCCACGTCAGCTAAGACATTGCCT-3′,5′-AGGCAATGTCTTAGCTGACGTGGGTTT-3′ were used to generate the Y61A mutation. The PCR products were immediately *Dpn*I (Roche) treated for 45 min to degrade template DNA, and transformed into *E. coli* ER2566. Mutations were confirmed by sequencing at the Robarts DNA Sequencing Facility (London, Ontario). Mutant proteins were purified as described above.

Mass Spectrometry. Electrospray mass spectra were recorded on a Micromass LCT time-of-flight mass spectrometer operating in the positive ion mode. Stock Isd protein solutions, in 1× phosphate-buffered saline (PBS) buffer (pH 7), were concentrated using centrifuge concentration tubes (Millipore) to approximately 1−2 mM. G-25 size exclusion columns (14 cm long, 1.5 cm diameter) were used for buffer exchange to ammonium formate (pH 7.3). Approximately 0.25 mL of concentrated protein in PBS was added to the column and eluted with the ammonium formate buffer. Samples were collected in small fractions, placed on ice, and analyzed within 30 min following preparation. To denature the proteins, small aliquots of 3 M formic acid were added (to bring the pH to approximately 2.3) prior to injection into the mass spectrometer. To refold rIsdE, a 500 μL sample of the acidified rIsdE solution was then placed on a G-25 size exclusion column, equilibrated with 20 mM ammonium formate (pH 7.2). The clear eluent was collected in fractions. Each fraction was then injected into the mass spectrometer, monitoring for peaks near 2000 m/z.

Spectroscopic Techniques. Absorption spectra were recorded on a Cary 500 UV−visible spectrophotometer (Varian Inc. Canada). MCD spectra were recorded using an SM2 5.5 T superconducting magnet (Oxford Instruments Ltd, Oxford, UK) in a J-820 CD spectropolarimeter (Jasco Inc., Japan). UV−visible absorption and MCD spectral data were recorded on identical solutions immediately following chemical changes at room temperature. The pyridine hemochrome test was used to determine the concentration of the heme, as described in Berry et al. (*14*). Protein concentrations were calculated using a molar extinction coefficient of 19 890 M^{-1} cm^{-1} for IsdE. Protein samples were diluted with 1× PBS to obtain absorbances in the B region of less than 0.8 in a 1 cm cuvette. Crystalline aliquots of sodium fluoride, sodium azide, and sodium cyanide were then added at approximately 5×, 10×, and 25× protein concentration and then at very large excess, as needed to obtain constant absorption and MCD spectra. The solutions were measured over a period of 1−2 h to ensure no further changes took place. To form the ferrous heme species, protein solutions were treated with increasing amounts of crystalline sodium hydrosulfite ($Na_2S_2O_4$) as the reducing agent until no further changes in

the absorption and MCD spectra were observed. To study carbon monoxide binding, gaseous CO was bubbled slowly into the sealed protein solutions through a serum cap until no further changes in the absorption spectrum were measured. UV−visible absorption spectra of protein solutions containing sodium hydrosulfite were obtained before and after MCD measurements to ensure reoxidation did not occur. To denature rIsdE, small aliquots of 3 M formic acid were added to reach a pH of 2.5. The absorption spectrum was measured immediately from 300 to 700 nm. Aliquots of 3 M ammonium hydroxide were then added to raise the pH to 7.5 to refold the protein.

The Role of MCD Spectroscopy in Studies of Heme Proteins. MCD spectroscopy provides information about the ground and excited-state orbital degeneracies of medium to high-symmetry complexes based on the Faraday A, B, and C terms (*15*). Key to the analysis of MCD spectral data is that the MCD bands lie at the same energy and exhibit approximately the same bandwidth as the absorption bands. In metalloporphyrins, the visible region absorption spectrum is dominated by two major electronic bands arising from $\pi \uparrow \pi^*$ transitions. In decreasing energy, we find the Soret (or B) band between 390 and 430 nm, Q_{vib} or β (a strong vibronic band progression) near 500 nm, and Q_{00} or α near 550 nm. The band maxima and relative intensities are characteristic of the oxidation and spin state of the central iron. Overlaid on these three bands are charge-transfer transitions between the central metal and the ring, which occur in the same spectral region (*15*). Charge-transfer transitions are particularly sensitive to the oxidation and spin state of the central iron being observed at different but characteristic wavelengths in the visible and near-IR regions. In the MCD spectrum of heme proteins, we find derivative-shaped Faraday A terms for species with degenerate excited states and nondegenerate ground states, and only positive A terms (positive lobe to high energy of the crossover energy) are observed. This will generally be the case for low spin ferrous hemes such as that coordinated by CO. B terms are Gaussian-shaped bands that arise from interactions between all adjacent states and can be both positively and negatively signed. C terms arise from ground state degeneracy and give rise at room temperatures to Gaussian-shaped bands of either sign and are temperature dependent. In heme, ground state degeneracy is found for high spin ferrous and all spin states of the ferric oxidation state. In addition, pseudo-A terms may be seen when two, oppositely signed C terms exist closely in energy. These pseudo-A terms may be of either sign. In the heme proteins, the MCD spectrum of five-coordinate, high spin ferrous heme provides an example of a Soret band region characterized by a pseudo-A term (*15*).

Because of inherent sensitivity to the electronic structure of the protoporphyrin IX, the iron, and its axial ligand(s), and because these effects have been shown to be systematic across a large number of proteins, the MCD spectral bands are diagnostic of the axial ligand identity, and the spin and oxidation state of the iron, allowing in many cases unambiguous determination of each of these parameters from room temperature measurements. This diagnostic sensitivity has been used widely and successfully to interrogate the spin, oxidation, and ligation state of the heme in a wide range of heme proteins, for example (*15*−*19*).

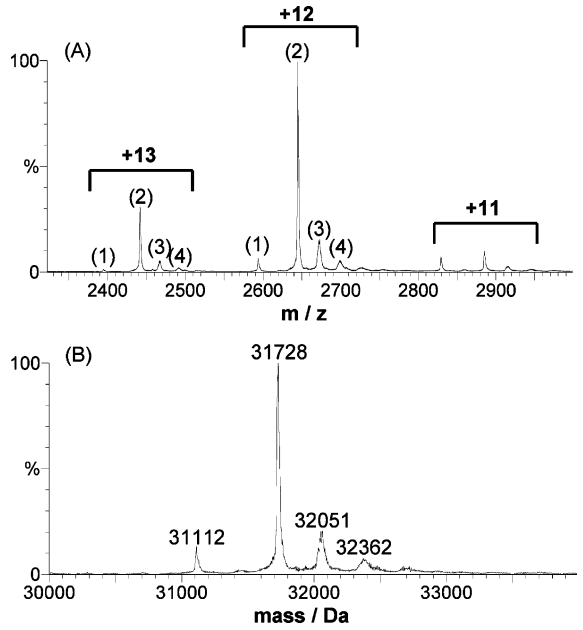

FIGURE 1: Charge state and mass spectra of rIsdE as purified from *E. coli*. (A) Charge state spectrum showing the +11, +12, and +13 charge states of rIsdE. No significant charge states were observed below 2300 m/z. (B) Deconvoluted mass spectrum shows four peaks corresponding to ligand-free rIsdE (31 112 Da), a single heme bound to rIsdE (31 728 Da), rIsdE bound to a single heme and a single unidentified ligand of approximately 323 Da (32 051 Da), and rIsdE bound to a single heme and a ligand of approximately 634 Da (32 362 Da).

RESULTS

rIsdE:Ligand Stoichiometry. Following purification from *E. coli*, rIsdE produced a reddish-brown solution, a feature common among heme-containing proteins. The charge state ESI-mass spectrum of rIsdE (Figure 1A) showed a group of charge states centered on +12. Deconvolution of those states gave four distinct masses (Figure 1B). The theoretical mass of rIsdE is 31 111 Da; thus, the peak at 31 112 Da represents heme-free rIsdE. The intense peak at 31 728 Da represents a single heme of mass 616 Da bound to the rIsdE (theoretical mass is 31 726 Da). We propose that the peaks at 32 051 and 32 423 Da arise from liganded reduced glutathione (GSH) with a measured mass of approximately 320 Da (theoretical mass 306.1 Da) and its oxidized form, glutathione-S−S-glutathione (GSSG) with a measured mass of 634 (theoretical mass 610.0). The weak signals contribute to the larger errors in mass determination of both the GSH and GSSG. These four peaks, shown in Figure 1B, were consistently observed for multiple spectral analyses of different rIsdE samples.

Reduction of the pH, which denatured the rIsdE, resulted in loss of the GSH and GSSG, indicating that these two species were bound as ligands to the protein. The charge state spectrum of rIsdE (neutral pH) is presented in Figure 2A. Following addition of formic acid, which lowered the pH to 2.3, a shift in the charge state distribution was observed (Figure 2B). Initially dominated by the +11, +12, and +13 charge states, acidifying the solution resulted in two distributions centered on +37 and separately on +22, suggesting that these forms of rIsdE were in an unfolded state (*20*, *21*). Isolation of these higher charge states revealed that at this low pH, rIsdE is free of both the heme, the GSH and GSSG,

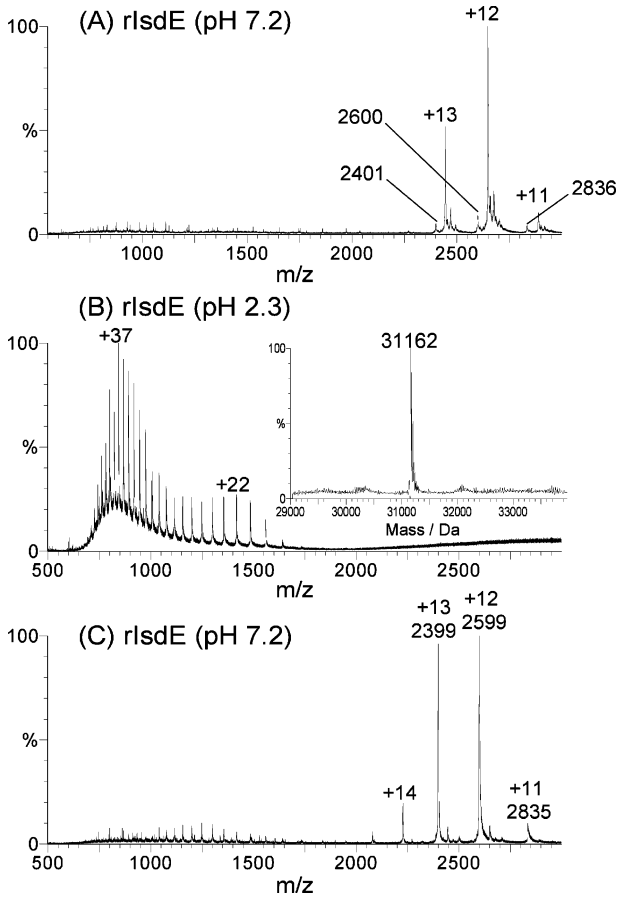

FIGURE 2: Charge state spectra of rIsdE monitoring protein folding. (A) Charge state spectrum of rIsdE as purified from *E. coli*. (B) Charge state spectrum of rIsdE at pH 2.3. (B inset) Deconvoluted mass spectrum of rIsdE at pH 2.3. (C) Charge state spectrum of rIsdE following neutralization (pH 7.2) of the acidified sample.

a result to be expected for an unfolded protein. The deconvoluted mass spectrum showed a single peak at 31 162 Da (Figure 2B inset), very close to the theoretical mass of 31 111 Da. This result showed that the peaks observed in the original rIsdE mass spectrum all arose from ligands bound to the same protein molecule. Cleavage products that can produce proteins of slightly different masses were, therefore, not present. The charge state spectrum obtained for a low pH rIsdE solution following elution from a G-25 size exclusion column, using ammonium formate buffer at pH 7.2, is shown in Figure 2C. The reappearance of the +11 to +14 charge states envelope indicates that rIsdE has returned to its native conformation. The major species present in the reneutralized sample is heme-free rIsdE (Figure 2C), as indicated by the intensification of the heme free rIsdE charge states at 2399, 2599, and 2835 m/z, although trace amounts of heme-bound rIsdE are still present (compared with the large fraction shown in Figure 2A). The small amount of ligand bound rIsdE can be attributed to the fact that rIsdE refolded near the top of the column, a location where the small ligands and large protein had only partially resolved. Once refolded, the presence of a small concentration of ligand in the direct environment, therefore, led to a small degree of binding.

This unfolding and refolding reaction of rIsdE is supported by the UV−visible absorption data presented in Figure 3. Under native conditions (~pH 7.3), the heme B band of rIsdE

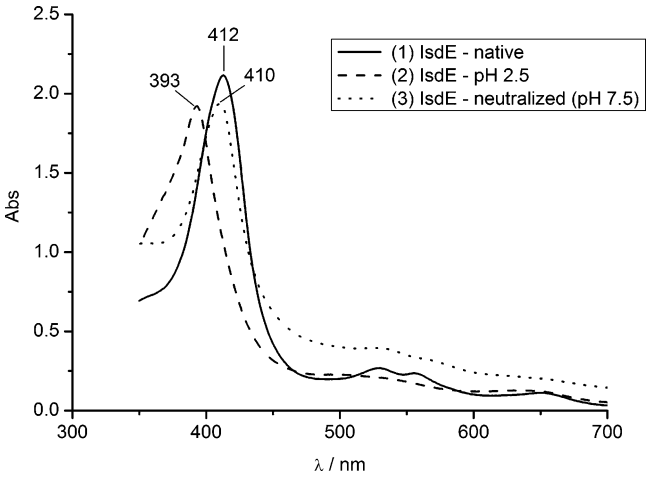

FIGURE 3: B band absorption spectra of rIsdE monitoring protein folding. (1) As purified from *E. coli*. (2) Following acidification of 1 to pH 2.5. (3) Following neutralization of 2 to pH 7.5.

is observed at 412 nm. Addition of formic acid to pH 2.5 results in a blue shift in the B band to 393 nm, which is characteristic of unbound heme (*22*). Upon neutralization of the acidic solution to pH 7.5, the B band returned close to its original position at 410 nm. These results indicated that upon acidification, the bound heme was released by the protein. Upon neutralization, the protein refolded and rebound the heme present in solution, giving the 410 nm absorption band. The 2 nm shift may have been due to the presence of a slightly different fraction of ferric and ferrous hemes bound to the rIsdE following refolding.

Heme Binding in rIsdE. We approach the determination of the properties of the bound heme in two parts. First, identification of the oxidation and spin status of the heme iron in the native protein, and second, identification of the ligation status of the iron, which leads to proposals for both proximal and distal ligands.

On the basis of analysis of the MCD spectra of the heme bound to rIsdE in the cell lysate, rIsdE was previously reported to contain a mixture of ferric and ferrous hemes (*10*). The MCD spectra described here of purified rIsdE offers further support for this conclusion and shows that the ferric heme is high- or intermediate-spin and definitively that the ferrous heme is low-spin. The analyses described below shows that a combination of multiple heme species gave rise to the complex absorption and MCD spectra presented in Figure 4A. The overall pattern of the absorption bands in Figure 4A closely resembles those of a low spin ferrous heme (*19*). Absorption spectra of low-spin ferrous hemes typically contain two well-defined bands in the visible region, corresponding to the Q_{00} and Q_{vib} transitions. In rIsdE these were observed at 558 and 530 nm, respectively. A third band was also always observed far to the red near 650 nm. This band may arise from (i) the photooxidation of PPIX (*23*, *24*), (ii) a charge-transfer band (*25*), or (iii) an electronic transition in the unidentified ligand. However, because the band maximum changed only by a few nanometers following the addition of sodium cyanide, sodium dithionite, and carbon monoxide (Figure 4) we have tentatively assigned it to charge-transfer that arises with both ferrous and ferric heme. Provisionally we identify the fifth position imidazole as the source because this band is not observed for the His229Ala mutant, comparing Figure 4A with 7A. It is possible that

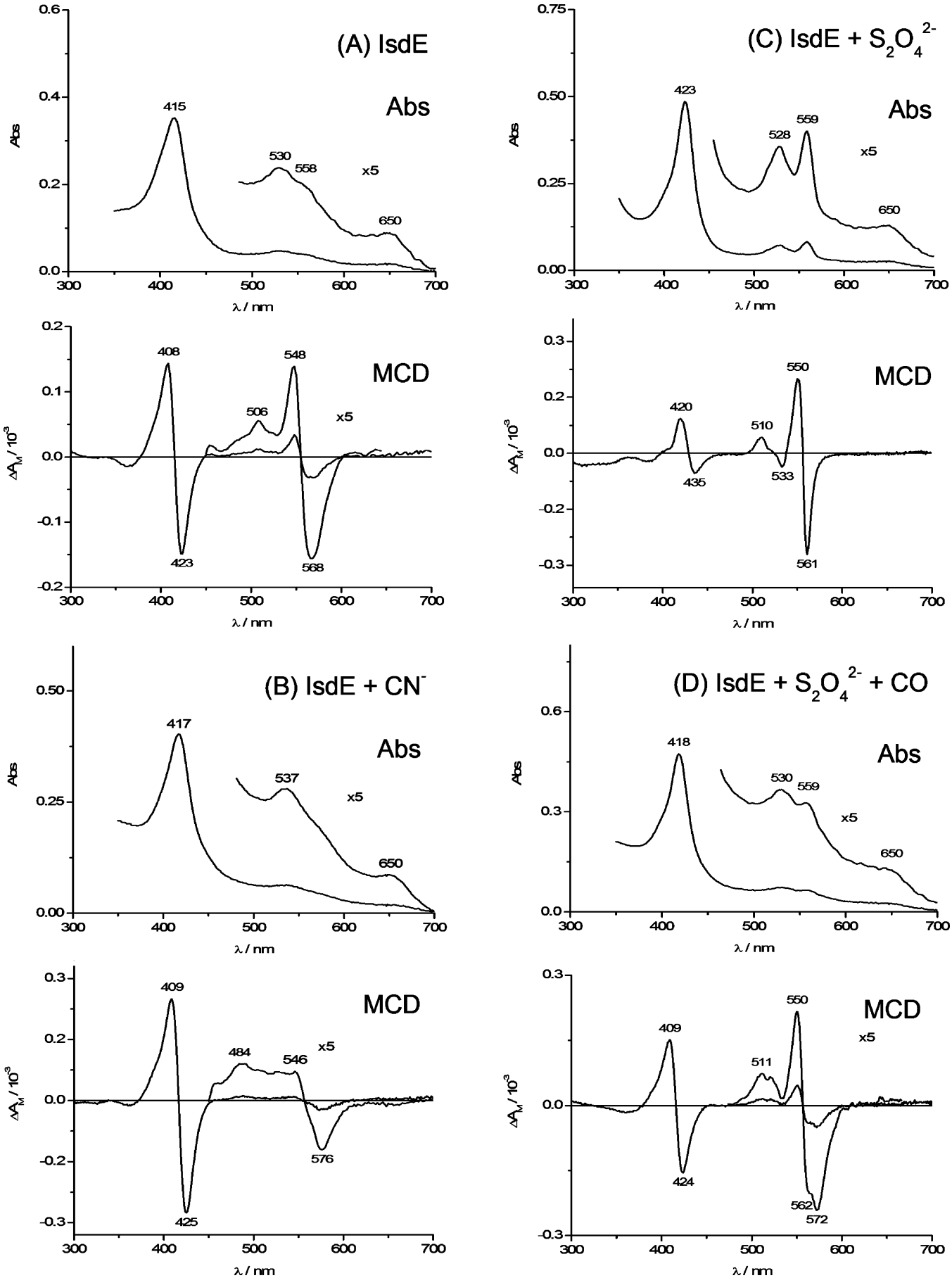

FIGURE 4: Absorption and MCD spectra of rIsdE. (A) As purified from *E. coli*. (B) Following the addition of crystalline sodium cyanide. (C) Following the addition of crystalline sodium hydrosulfite. (D) Following the addition of crystalline sodium hydrosulfite and carbon monoxide. Reagents were added to samples of rIsdE until no further changes were observed in the absorption spectra.

the band is actually a composite of bands connected with the presence of the sixth position methionine in the ferrous and solely the histidine in the ferric heme.

While the absorption spectrum of rIsdE appears to arise solely from low-spin ferrous heme, the MCD spectrum of rIsdE shown in Figure 4A is quite different when compared with spectral data for well-characterized low-spin ferrous heme species for myoglobin (*19*) and cytochrome c (*26*). Particularly, the large intensity ratio between the B and Q bands for rIsdE (approximately 5:1) is much larger than previously reported (usually closer to 2:1 or less) (*19*, *27*). Those reports, however, were based on protein solutions containing a single heme species. Analysis of these spectral properties, therefore, indicates that rIsdE contains both ferric and low-spin ferrous hemes; thus, the abnormally large B:Q intensity ratio results from the overlap of a ferric heme A term with an A term from a low-spin ferrous heme, effectively adding to the intensity in this region of the MCD spectrum.

Coordination of a strong field ligand, such as cyanide, to heme results in the formation of a low-spin iron center (*19*, *28*). Examination of the MCD spectrum from a myoglobin heme model shows that upon binding of cyanide, two main features are observed, (1) a negative band near 580 nm appears, and (2) an increase in the B:Q-band intensity ratio (*19*). These features were both observed for rIsdE with the appearance of a negative band at 576 nm, and an increase in the B:Q-band intensity ratio from 5:1 to approximately 10:1 (Figure 4B). The addition of a reducing agent to rIsdE produced a significant drop in the B band intensity, with the B:Q-band intensity ratio changing from 5:1 to 1:3 (Figure 4C). The overall band pattern closely resembles that of ferrous heme with bis-tetrahydrothiophene ligation (*27*). The addition of carbon monoxide to the reduced solution then brought back the B band intensity (Figure 4D), indicating that the CO had bound to the Fe(II). The double band appearing at 562 and 573 nm was a result of the incomplete ligation of carbon monoxide. Figure S1 illustrates that with increasing amounts of carbon monoxide the 572 nm band increases in intensity while the 562 nm band decreases. Vigorous addition of carbon monoxide could not entirely eliminate this dual peak, suggesting that carbon monoxide ligation was hindered, possibly due to bis-axial ligation of the ferrous heme, as is suggested by the reduced-heme rIsdE MCD spectrum. Collectively, the mass and MCD spectral data, Figures 1 and 4, show that a single rIsdE protein molecule binds either a single ferric heme (of either high or intermediate spin state) or a single low-spin ferrous heme. The ferrous heme is partially blocked from small ligands. The ferric heme, however, is readily accessible to anionic ligands such as cyanide. Additionally, we have identified the distal ligand of the ferrous fraction as being methionine, due to the similarity in the reduced rIsdE MCD spectrum to neutral thiol coordinated heme.

Mutational Analysis of rIsdE. IsdE is a member of the metal chelate superfamily of ligand binding proteins. The overall fold of the protein in this superfamily is well-conserved and is composed of two domains, each consisting of a central β-sheet and surrounding α-helices, linked by an α helix that spans the length of the protein. The substrate binding site is in a cleft formed between the two α/β domains (*29*, *30*). Despite the lack of crystal structure information on heme binding proteins in the metal chelate binding protein superfamily, the structural conservation in this protein superfamily allowed us to generate a model of IsdE using structural data from the *E. coli* periplasmic binding proteins BtuF and FhuD (*31*−*33*). The model indicated several potential heme ligands situated in the predicted heme binding cleft. Site-directed mutagenesis was used to introduce point mutations into rIsdE by replacing the native residue with alanine, so that the functions of these residues could be examined. Tyrosines were targeted because of the known heme-iron tyrosyl ligation in the Isd NEAT domain structures (*4*, *5*). Mutation of Y61, Y187, and Y261, the three tyrosine residues believed to be in the rIsdE heme binding site, did not significantly alter the results compared to those of native rIsdE. For example, the charge state spectrum for rIsdE Y261A showed that the +12, +13 charge states still dominated (data not shown), indicating that the overall fold of the protein was not affected by the mutation (*20*, *34*). A strong single heme bound signal and two weaker signals approximately 320 and 640 Da higher than the heme bound peak were also observed. The absorption and MCD spectra were identical to those of the native rIsdE shown in Figure 4. Collectively, the data suggest that Y61, Y187, and Y261 do not participate directly in heme binding and the alanine substitutions did not change the conformation of the native protein.

Since histidine is a common heme-iron ligand, and one histidine, H229 projected into the binding pocket in our model, we next targeted this residue. In contrast to what we observed for the tyrosine mutants described above, mutation of H229 resulted in significant changes in both the mass and MCD spectra of the mutant protein. The mass spectrum of rIsdE H229A (Figure S2C) clearly shows that only heme free (31,097 Da) and heme-bound protein (31,741 Da) were present. There is no signal where, in the native rIsdE, two additional peaks are observed. Again the +12 and +13 charge states dominated the spectrum, suggesting that the changes observed were due to the lack of an imidazole side group at amino acid 229 and not an alteration in the fold of the protein (*20*, *34*).

The MCD spectrum of rIsdE H229A closely resembled that of a low-spin ferrous heme (Figure 5A) with THT and NO in the axial positions (*27*). rIsdE bound to a single heme should be represented by a peak at 31 713 Da in the mass spectrum. However, the peak is observed at 31 741 Da, a difference of 28 Da. Thus, it appears that the ferrous heme in rIsdE H229A binds NO during purification, even though no external source was provided. The two A terms, with crossover points at 421 and 576 nm, along with the positive B term at 519 nm fit the band pattern of a low-spin ferrous heme very closely (*19*). Previously it was observed in the MCD spectrum of native rIsdE that cyanide did bind but for rIsdE H229A, no change was observed following addition of excess cyanide (Figure 5B). The addition of a reducing agent did produce minor changes; however, these were most likely due to some ferric heme contamination (Figure 5C). This suggests that there is a very small fraction of ferric heme in rIsdE H229A unlike the case with the native protein, and the majority of the heme was low-spin ferrous.

A rIsdE double mutant containing the Y61A and H229A mutations did not show any change following reduction (Figure 6). It appears that Y61 may play a small role in

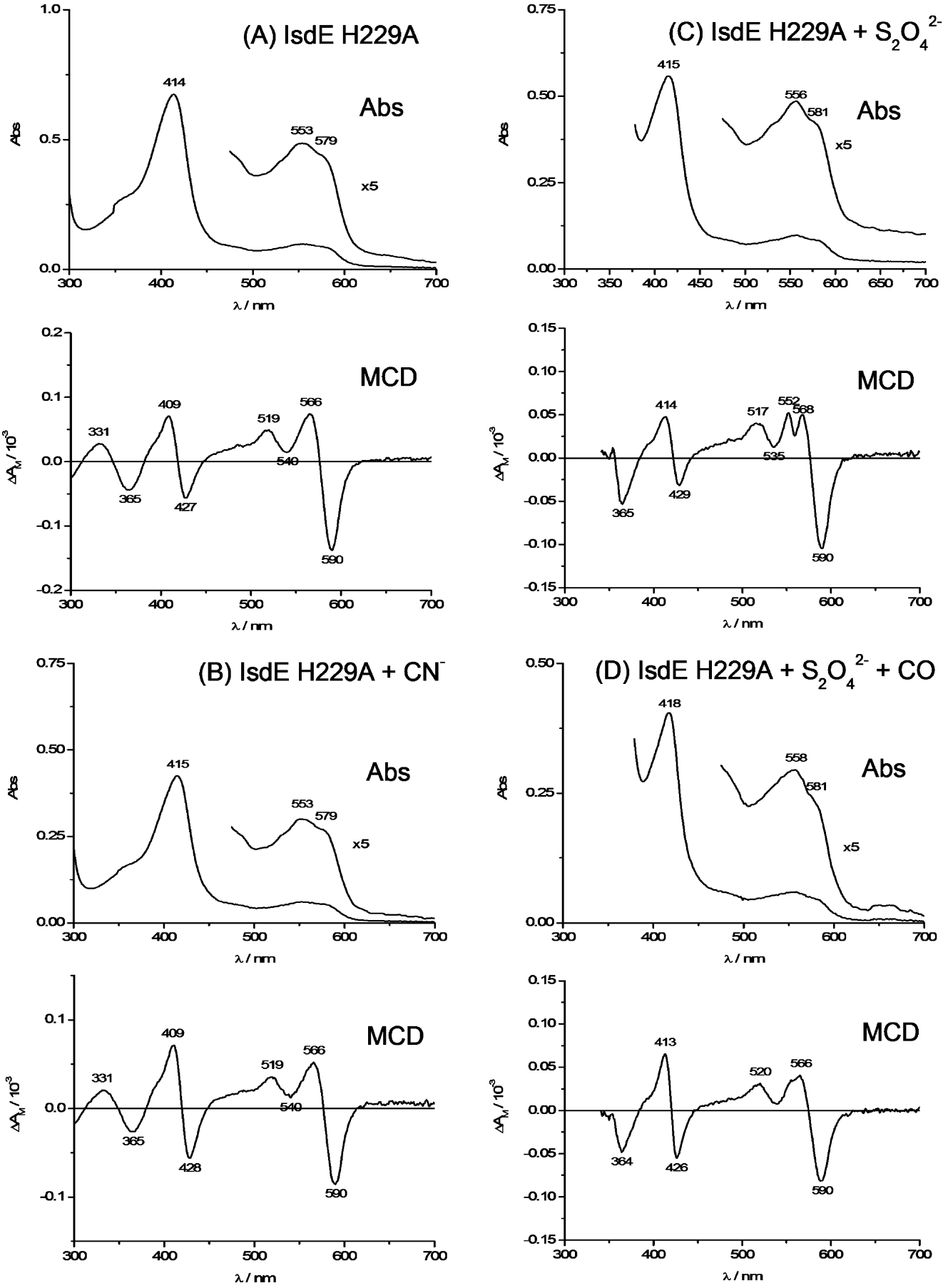

FIGURE 5: Absorption and MCD spectra of rIsdE H229A. (A) As purified from *E. coli*. (B) Following the addition of crystalline sodium cyanide. (C) Following the addition of crystalline sodium hydrosulfite. (D) Following the addition of crystalline sodium hydrosulfite and carbon monoxide.

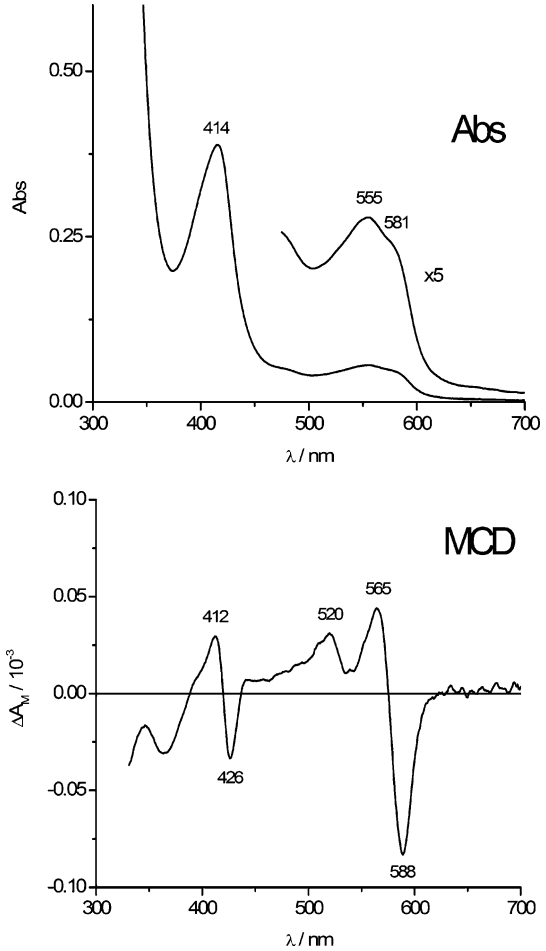

FIGURE 6: Absorption and MCD spectra of rIsdE Y61A/H229A following the addition of sodium hydrosulfite.

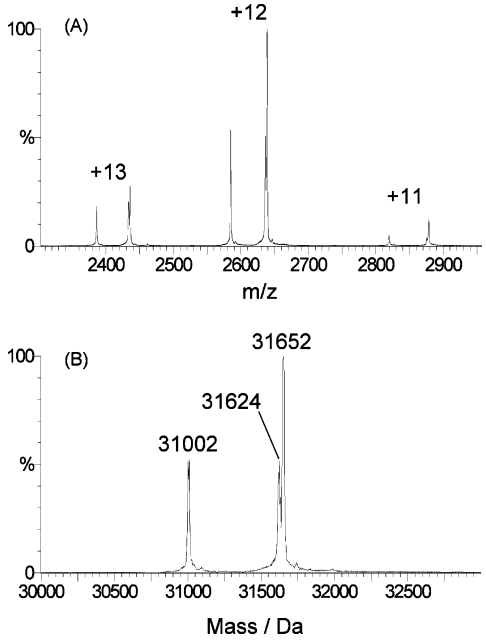

FIGURE 7: Charge state and deconvoluted mass spectrum of rIsdE Y61A/H229A. (A) Charge state spectrum showing the characteristic +11, +12, and +13 rIsdE charge states. (B) Deconvoluted mass spectrum showing heme-free (31 002 Da), single heme bound (31 624 Da), and single heme with NO or CO in the distal position (31 652 Da) rIsdE Y61A/H229A.

coordinating ferric heme in rIsdE and upon elimination of only H229A, a small amount still remains bound. The mass spectrum of the Y61A/H229A rIsdE double mutant also showed the presence of a NO liganded heme, as indicated by the peak at 31 652 Da (Figure 7B). Overall, the spectral band patterns remained in close agreement to that of a low-spin ferrous heme. Following the addition of CO, no change was observed (Figure 5D). It is interesting to note that none of the rIsdE mutants containing the H229A mutation exhibited an absorption band at 650 nm. This leads to the conclusion that the band near 650 nm (the band maximum moves 4−5 nm depending on the oxidation and spin state in all other mutants and the native) arises from charge transfer from the His proximal ligand to the iron. Overall, the data for rIsdE H229A suggest that a methionine residue binds a low-spin ferrous heme, with a strong π-acceptor ligand in the distal site. The binding of small ligands is more favorable than is the case with native rIsdE due to the removal of H229. Therefore, in the native state, H229 and a methionine residue coordinate to the heme in rIsdE.

All of the data for rIsdE containing the H229A mutation showed that only low-spin ferrous heme was bound. To investigate if ferric heme could also bind in the heme site, a strong oxidizing agent (ferricyanide) was added to samples of native rIsdE and rIsdE Y61A/H229A. Following addition of the oxidizing agent and purification on a G-25 size exclusion column, the charge state spectrum of oxidized rIsdE showed no change (Panels A and B of Figure 8). A strong single heme bound peak and weak GSH and GSSG peaks were still present. In the rIsdE Y61A/H229A double mutant a marked reduction in the degree of heme binding was observed. Preceding ferricyanide addition (Figure 8C) approximately 60−70% of the protein was bound to heme. This value significantly dropped to less than 10% following oxidation (Figure 8D).

DISCUSSION

The proposed sequence of events in heme acquisition by *S. aureus*, through the Isd system, is that hemeproteins such as hemoglobin are bound by IsdB or HasA/IsdH, heme is then removed to be bound by IsdA, and then heme passes through IsdC before being bound by the ABC transporter, IsdEF, at the cell membrane (*1*). Once in the cytoplasm, heme may be degraded by the action of IsdG and IsdI (*6*). The coordination of the hemes in IsdA and IsdC have previously been reported (*4*, *5*) but they involve the NEAT domain (*35*), whereas IsdE does not possess a NEAT domain. IsdE is a lipoprotein which functions as a high-affinity ligand binding protein. It is also predicted to associate with the IsdF ABC transporter permease. Questions that have remained unanswered currently concern the heme binding properties, namely the number of hemes bound, their oxidation and spin state, and the amino acids in the binding site that coordinate the heme. The data reported here provide that information and allow specific conclusions to be drawn concerning the structural properties of the heme binding site. When examining the data for rIsdA (*9*, *10*, *36*), rIsdC (*5*, *24*, *36*), and rIsdE, there are several common themes. One is the ability of each protein to bind heme. The other is the presence of ligands at approximately 300−320 and 610−630 Da in mass. Because of the multiple purification steps preceding mass spectral analysis, it is unlikely that any compound not bound to the protein would still be present. The mass spectrum of

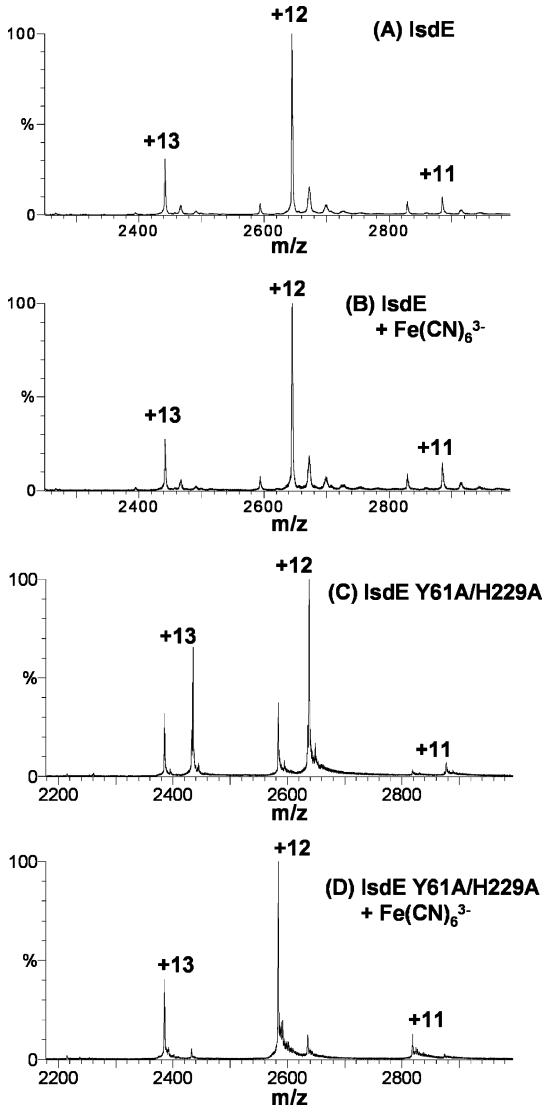

FIGURE 8: Charge state spectra of rIsdE (A, B) and rIsdE Y61A/H229A (C, D) preceding and following the addition of ferricyanide.

rIsdE at low pH (unfolded) in Figure 2B clearly shows that only ligand-free protein is present at 31 162 Da providing strong evidence that these unidentified peaks in the mass spectrum measured at neutral pH do not arise from the presence of a slightly heavier protein impurity (for example arising from imperfect cleavage). The masses strongly suggest the presence of a minor fraction of GSH and GSSG bound to the rIsdE at neutral pH, but which is released at low pH when the protein is denatured.

Mack et al. have previously reported that cell lysates containing overexpressed rIsdE exhibited MCD spectra that suggested the presence of both ferric and ferrous hemes (*10*). The MCD data of purified rIsdE described here confirm those previous conclusions and provide more details of both the spin states and the structure of the binding sites. The ESI-MS data show conclusively that rIsdE binds only one heme. The observation of both ferric and ferrous hemes means that binding of either oxidation state of the heme-iron is possible.

The MCD spectra of low spin ferrous hemes are quite simple to analyze because of a lack of charge-transfer bands in the 400−700 nm region. Three features are observed: two A terms corresponding to the B_{00} and Q_{00} absorption bands and a positive peak to the blue of the Q-band A term (*19*). The MCD spectrum of rIsdE (Figure 4A) follows this band pattern with only slight differences, suggesting that the predominant heme species present is low-spin ferrous heme. An abnormally large B:Q A-term intensity ratio and the appearance of overlapping bands in the visible region separate the MCD spectrum of rIsdE from those of other low-spin ferrous heme-containing proteins. These anomalies can be explained by the presence of ferric heme as a fraction of the total bound heme. Ferric hemes contain numerous charge-transfer bands in the visible region (*16*, *19*, *37*), which may explain the complex rIsdE MCD spectrum observed in this region. In myoglobin, carbon monoxide binding to ferrous heme gives a 2:1 B:Q-band A term intensity ratio in the MCD spectrum (*19*). Oxygen binding gives an approximate 1:3 ratio. Ferric heme A-terms show similar structure to those of low-spin ferrous hemes in the B region. Thus, the overlap between ferrous and ferric signals will result in the increased intensity observed.

Since the pure ferric heme rIsdE is unavailable, the determination of the ferric heme spin state was difficult. The presence of ferric heme is shown in the MCD spectral changes observed following the addition of ligands (CN^-) and a reducing agent ($Na_2S_2O_4$) (Figure 4). Cyanide coordinates much stronger with ferric heme than with ferrous heme. The appearance of low-spin ferric heme signals following cyanide addition, therefore, suggests that ferric heme with a high or intermediate spin state was initially present. Confirmation also comes from the changes observed following the addition of sodium hydrosulfite. If only ferrous heme were present, one would expect no change in the MCD spectrum. This, however, is not the case. The original ferric heme in rIsdE is reduced upon addition of sodium hydrosulfite, so that an MCD spectrum characteristic of a low-spin ferrous heme with methionine and histidine axial ligands is measured (*26*, *27*). Cyanide addition was shown to coordinate the ferric heme, so when reduced to ferrous, coordination by a small ferrous binding ligand would be expected to still occur. Indeed, the addition of carbon monoxide to a reduced solution of rIsdE results in an MCD spectrum characteristic of low-spin ferrous heme (Figure 4D) with His and CO as axial ligands (*19*). The overlapping signals observed in the Q region (as shown by the peaks at 562 and 572 nm) can be understood in terms of the increased affinity for methionine to the ferrous heme so that CO ligation becomes hindered.

The band appearing at 650 nm in the absorption spectra of rIsdE (Figure 4A) offers evidence of a high-spin ferric state. Heme bands this far to the red are rather rare but have been observed in cytochrome c peroxidase (*25*). Yonetani et al. have assigned this band to a charge-transfer transition in a high-spin ferric heme (*25*). Initially, we concluded that its persistence in all of the rIsdE species from their MCD spectra presented in Figures 4 and 7 suggests that just high spin ferric heme was not the only cause. Although there are a number of species that can cause a band near 650 nm, the absence of the 650 nm band only with the His229 mutant convinces us that the only explanation can be charge transfer from His 229. We can eliminate as a cause of the 650 nm peak the products of PPIX photo-oxidation (*23*, *24*), because in none of the rIsdE mass spectra recorded were peaks corresponding to PPIX (mass 562.7 Da) or bilirubin (mass

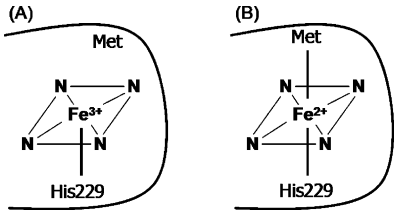

FIGURE 9: Model of the IsdE heme binding pocket, illustrating (A) ferric heme binding and (B) ferrous heme binding.

584.7 Da) (free in solution or bound to rIsdE) observed, and we can also eliminate the result of GSH binding because the GSH identified in the ESI-MS is present in such a small fraction that the absorbance would not be observed.

A series of alanine substitution mutations in the vicinity of the heme binding site were made. Of these, H229A clearly exhibited spectral data different from the native protein. The mass spectrum of rIsdE H229A clearly shows that it only binds a single heme and that very little protein is heme-free (Figures 6). MCD spectra for the series of liganded species then confirm that the heme present is low-spin ferrous (Figures 7A). There was no change observed in the MCD spectrum following the addition of cyanide and carbon monoxide. This is most likely a result of ligation by a methionine residue of the protein and by NO, as would be expected from the presence of a low-spin ferrous iron. Protein bound ferrous hemes, containing water or an open distal position, show readily recognizable high-spin characteristics, as observed in myoglobin (*19*).

The MCD spectrum of rIsdE H229A (Figure 5A) clearly shows that the ferrous heme bound in rIsdE is low-spin. The data suggest that H229 binds heme near the edge of the heme binding pocket. This location would leave bound heme relatively exposed to the environment, which helps to explain the observed ligation of cyanide and carbon monoxide (when reduced). The results indicate that both ferric and ferrous heme can coordinate in the native rIsdE. However, upon elimination of H229, coordination of ferric heme did not occur. The charge state spectra of rIsdE in Figure 8 show that following the addition of an oxidizing agent, no change is observed. However, the charge state spectra of rIsdE Y61A/H229A show that heme binding is greatly reduced following the addition of ferricyanide.

In the ferric state, His229 coordinates the heme in the proximal site, with a methionine residue near the distal position. Because of the lowered affinity of methionine for ferric heme, cyanide can ligate any ferric heme present. In the ferrous state, the distal methionine now coordinates much more tightly to form the low-spin ferrous state (Figure 9). It is interesting to note that a methionine residue in the distal heme site can function as a means for rIsdE to distinguish between the ferric and ferrous oxidation states. Addition of CO can replace the Met ligand. These observations suggest that rIsdE contains two different heme iron coordination modes in the same site, one for ferric and the other for ferrous hemes. Mutation of H229 leaves only methionine coordination to the heme. Thus upon oxidation, the heme binding affinity is greatly reduced and, therefore, heme does not bind.

In summary, rIsdE can bind different heme molecules but only one at a time. In this study, we found that a small fraction of rIsdE binds one ferric heme (spin state is either high or intermediate), while a larger fraction binds one ferrous heme, which is low-spin; in both cases we found that a molecule of GSH and GSSG was also bound to the protein. Our studies indicate that the bound heme is held near the edge of the heme binding pocket by H229 and a methionine residue. Binding in a shallow pocket in which substrate is held near the edge of the protein is consistent with other members of the metal chelate superfamily of substrate binding proteins.

Addendum. It is noted that during the time of review of this manuscript, the structure determination of *S. aureus* IsdE in complex with heme was reported (*38*). Our data on the properties of the heme-bound form of the protein *in solution* are in complete agreement with the heme protein association revealed by the crystal structure, which identifies the heme-coordinating methionine proposed here as residue Met78.

ACKNOWLEDGMENT

D.E.H. is a member of the Infectious Diseases Research Group at UWO, and M.J.S. is a member of the Centre for Chemical Physics at UWO. D.E.H. and M.J.S. acknowledge operating support from the Natural Sciences and Engineering Research Council of Canada. We thank Mr. Doug Hairsine, Department of Chemistry, for help with the mass spectrometry.

SUPPORTING INFORMATION AVAILABLE

Two figures (S1 and S2) that show the spectroscopic changes with addition of CO to ferrous IsdE and the mass spectra data for the H229A mutant. This material is available free of charge via the Internet at http://pubs.acs.org.

REFERENCES

1. Mazmanian, S. K., Skaar, E. P., Gaspar, A. H., Humayun, M., Gornicki, P., Jelenska, J., Joachmiak, A., Missiakas, D. M., and Schneewind, O. (2003) Passage of heme-iron across the envelope of *Staphylococcus aureus*, *Science 299*, 906−909.
2. Mazmanian, S. K., Ton-That, H., Su, K., and Schneewind, O. (2002) An iron-regulated sortase anchors a class of surface protein during *Staphylococcus aureus* pathogenesis, *Proc. Natl. Acad. Sci. U.S.A. 99*, 2293−2298.
3. Torres, V. J., Pishchany, G., Humayun, M., Schneewind, O., and Skaar, E. P. (2006) *Staphylococcus aureus* IsdB is a hemoglobin receptor required for heme iron utilization, *J. Bacteriol. 188*, 8421−8429.
4. Grigg, J. C., Vermeiren, C. L., Heinrichs, D. E., and Murphy, M. E. (2007) Haem recognition by a *Staphylococcus aureus* NEAT domain, *Mol. Microbiol. 63*, 139−149.
5. Sharp, K. H., Schneider, S., Cockayne, A., and Paoli, M. (2007) Crystal structure of the heme-IsdC complex, the central conduit of the Isd iron/heme uptake system in *Staphylococcus aureus*, *J. Biol. Chem. 282*, 10625−10631.
6. Skaar, E. P., Gaspar, A. H., and Schneewind, O. (2004) IsdG and IsdI, heme-degrading enzymes in the cytoplasm of *Staphylococcus aureus*, *J. Biol. Chem. 279*, 436−443.
7. Dryla, A., Gelbmann, D., von Gabain, A., and Nagy, E. (2003) Identification of a novel iron regulated staphylococcal surface protein with haptoglobin-haemoglobin binding activity, *Mol. Microbiol. 49*, 37−53.
8. Pilpa, R. M., Fadeev, E. A., Villareal, V. A., Wong, M. L., Phillips, M., and Clubb, R. T. (2006) Solution structure of the NEAT (NEAr Transporter) domain from IsdH/HarA: the human hemoglobin receptor in *Staphylococcus aureus*, *J. Mol. Biol. 360*, 435−447.
9. Vermeiren, C. L., Pluym, M., Mack, J., Heinrichs, D. E., and Stillman, M. J. (2006) Characterization of the heme binding properties of *Staphylococcus aureus* IsdA, *Biochemistry 45*, 12867−12875.

10. Mack, J., Vermeiren, C., Heinrichs, D. E., and Stillman, M. J. (2004) In vivo heme scavenging by *Staphylococcus aureus* IsdC and IsdE proteins, *Biochem. Biophys. Res. Commun. 320*, 781−788.
11. Maresso, A. W., Chapa, T. J., and Schneewind, O. (2006) Surface protein IsdC and Sortase B are required for heme-iron scavenging of *Bacillus anthracis*, *J. Bacteriol. 188*, 8145−8152.
12. Reniere, M. L., Torres, V. J., and Skaar, E. P. (2007) Intracellular metalloporphyrin metabolism in *Staphylococcus aureus*, *Biometals 20*, 333−345.
13. Skaar, E. P., Humayun, M., Bae, T., DeBord, K. L., and Schneewind, O. (2004) Iron-source preference of *Staphylococcus aureus* infections, *Science 305*, 1626−1628.
14. Berry, E. A., and Trumpower, B. L. (1987) Simultaneous determination of hemes a, b, and c from pyridine hemochrome spectra, *Anal. Biochem. 161*, 1−15.
15. Mack, J., and Stillman, M. J. (2003) in *Handbook of porphyrins and related macrocycles* (Kadish, K. M., Smith, K. M., and Guilard, R., Eds.), p 43, Academic Press, New York.
16. Browett, W. R., and Stillman, M. J. (1979) Magnetic circular dichroism studies of bovine liver catalase, *Biochim. Biophys. Acta 577*, 291−306.
17. Cheek, J., and Dawson, J. H. (2000) in *The handbook of porphyrins and related macrocycles* (Kadish, K. M., Smith, K. M., and Guilard, R., Eds.), pp 339−369, Academic Press, New York.
18. Springall, J., Stillman, M. J., and Thomson, A. J. (1976) Low temperature magnetic circular dichroism spectra of met- and myoglobin derivatives, *Biochim. Biophys. Acta 453*, 494−501.
19. Vickery, L., Nozawa, T., and Sauer, K. (1976) Magnetic circular dichroism studies of myoglobin complexes. Correlations with heme spin state and axial ligation, *J. Am. Chem. Soc. 98*, 343−350.
20. Cunsolo, V., Foti, S., Rosa, C. L., Saletti, R., Canters, G. W., and Verbeet, M. P. (2003) Monitoring of unfolding of metallo-proteins by electrospray ionization mass spectrometry, *J. Mass Spectrom. 38*, 502−509.
21. Konermann, L., and Douglas, D. J. (1997) Acid-induced unfolding of cytochrome c at different methanol concentrations: electrospray ionization mass spectrometry specifically monitors changes in the tertiary structure, *Biochemistry 36*, 12296−12302.
22. Gibson, G. H., and Antonini, E. (1963) Rates of reaction of native human globin with some hemes, *J. Biol. Chem. 238*, 1384−1388.
23. Ericson, M. B., Grapengiesser, S., Gudmundson, F., Wennberg, A.-M., Larko, O., Moan, J., and Rosen, A. (2003) A spectroscopic study of the photobleaching of protoporphyrin IX in solution, *Lasers Med. Sci. 18*, 56−62.
24. Pluym, M., Vermeiren, C. L., Mack, J., Heinrichs, D. E., and Stillman, M. J. (2007) Protoporphyrin IX and heme binding properties of *Staphylococcus aureus* IsdC, *J. Porphyrins Phthalocyanines 11*, 165−171.
25. Yonetani, T., Wilson, D. F., and Seamonds, B. (1966) Studies on cytochrome c peroxidase, *J. Biol. Chem. 241*, 5347−5352.
26. Risler, J. L., and Groudinshy, O. (1973) Magnetic circular dichroism studies of cytochrome c and cytochrome b_2, *Eur. J. Biochem. 35*, 201−205.
27. Perera, R., Sono, M., Sigman, J. A., Pfister, T. D., Lu, Y., and Dawson, J. H. (2003) Neutral thiol as a proximal ligand to ferrous heme iron: implications for heme proteins that lose cysteine thiolate ligation on reduction, *Proc. Natl. Acad. Sci. U.S.A. 100*, 3641−3646.
28. Housecroft, C. E., and Sharpe, A. G. (2005) *Inorg. Chem.*, Vol. 2, Pearson Education Limited, Essex, England.
29. Locher, K. P. (2004) Structure and mechanism of ABC transporters, *Curr. Opin. Struct. Biol. 14*, 426−431.
30. Locher, K. P., and Borths, E. (2004) ABC transporter architecture and mechanism: implications from the crystal structures of BtuCD and BtuF, *FEBS Lett. 564*, 264−268.
31. Borths, E. L., Locher, K. P., Lee, A. T., and Rees, D. C. (2002) The structure of *Escherichia coli* BtuF and binding to its cognate ATP binding cassette transporter, *Proc. Natl. Acad. Sci. U.S.A. 99*, 16642−16647.
32. Karpowich, N. K., Huang, H. H., Smith, P. C., and Hunt, J. F. (2003) Crystal Structures of the BtuF Periplasmic-binding Protein for Vitamin B12 Suggest a Functionally Important Reduction in Protein Mobility upon Ligand Binding, *J. Biol. Chem. 278*, 8429−8434.
33. Clarke, T. E., Braun, V., Winkelmann, G., Tari, L. W., and Vogel, H. J. (2002) X-ray crystallographic structures of the *Escherichia coli* periplasmic protein FhuD bound to hydroxamate-type siderophores and the antibiotic albomycin, *J. Biol. Chem. 277*, 13966−13972.
34. Yan, X., Watson, J., Ho, P. S., and Deinzer, M. L. (2004) Mass Spectrometric approaches using electrospray ionization charge states and hydrogen-deuterium exchange for determining protein structures and their conformational changes, *Mol. Cell. Proteomics 3*, 10−23.
35. Andrade, M. A., Ciccarelli, F. D., Perez-Iratxeta, C., and Bork, P. (2002) NEAT: a domain duplicated in genes near the components of a putative Fe3+ siderophore transporter from Gram-positive pathogenic bacteria, *GenomeBiology 3*, research0047.1−research0047.5.
36. Pluym, M., Muryoi, N., Heinrichs, D. E., and Stillman, M. J. (2007) Heme binding in the NEAT domains of IsdA and IsdC of *Staphylococcus aureus*, *J. Inorg. Biochem.*, submitted.
37. Browett, W. R., and Stillman, M. J. (1984) Temperature dependence in the absorption spectra of beef liver catalase, *Biophys. Chem. 19*, 311−320.
38. Grigg, J. C., Vermeiren, C. L., Heinrichs, D. E., and Murphy, M. E. (2007) Heme coordination by *Staphylococcus aureus* IsdE, *J. Biol. Chem.*

BI7009585